Cell

A Family of Protein-Deglutamylating Enzymes Associated with Neurodegeneration

Krzysztof Rogowski,[1,*] Juliette van Dijk,[1] Maria M. Magiera,[1,6,7,8] Christophe Bosc,[2] Jean-Christophe Deloulme,[2] Anouk Bosson,[2] Leticia Peris,[2] Nicholas D. Gold,[1] Benjamin Lacroix,[1] Montserrat Bosch Grau,[1,6,7,8] Nicole Bec,[3] Christian Larroque,[3] Solange Desagher,[4] Max Holzer,[5] Annie Andrieux,[2] Marie-Jo Moutin,[2] and Carsten Janke[1,6,7,8,*]
[1]CRBM, Université Montpellier 2 and 1, CNRS UMR 5237, Montpellier 34293, France
[2]INSERM U836, Grenoble Institut des Neurosciences, CEA-iRTSV-GPC, Université Joseph Fourier, Grenoble 38042, France
[3]CRLC Val d'Aurelle, Institut de Recherche en Cancérologie de Montpellier, INSERM, Montpellier 34298, France
[4]IGMM, Université Montpellier 2, CNRS UMR 5535, Montpellier 34293, France
[5]Paul-Flechsig-Institute of Brain Research, University of Leipzig, Leipzig 04109, Germany
[6]Present address: Institut Curie, Orsay 91405, France
[7]Present address: CNRS UMR 3306, Orsay 91405, France
[8]Present address: INSERM U1005, Orsay 91405, France
*Correspondence: krzysztof.rogowski@crbm.cnrs.fr (K.R.), carsten.janke@curie.fr (C.J.)
DOI 10.1016/j.cell.2010.10.014

SUMMARY

Polyglutamylation is a posttranslational modification that generates glutamate side chains on tubulins and other proteins. Although this modification has been shown to be reversible, little is known about the enzymes catalyzing deglutamylation. Here we describe the enzymatic mechanism of protein deglutamylation by members of the cytosolic carboxypeptidase (CCP) family. Three enzymes (CCP1, CCP4, and CCP6) catalyze the shortening of polyglutamate chains and a fourth (CCP5) specifically removes the branching point glutamates. In addition, CCP1, CCP4, and CCP6 also remove gene-encoded glutamates from the carboxyl termini of proteins. Accordingly, we show that these enzymes convert detyrosinated tubulin into Δ2-tubulin and also modify other substrates, including myosin light chain kinase 1. We further analyze *Purkinje cell degeneration* (*pcd*) mice that lack functional CCP1 and show that microtubule hyperglutamylation is directly linked to neurodegeneration. Taken together, our results reveal that controlling the length of the polyglutamate side chains on tubulin is critical for neuronal survival.

INTRODUCTION

Polyglutamylation is a posttranslational modification that generates glutamate side chains of variable length on the γ-carboxyl groups of glutamic acid residues within the primary sequence of the target proteins. This modification has been initially discovered on α- and β-tubulin, the building blocks of microtubules (MTs; Eddé et al., 1990; Rüdiger et al., 1992), and later also found on other proteins (Regnard et al., 2000; van Dijk et al., 2008). Polyglutamylation levels are particularly high on stable MT assemblies such as the ones found in neurons (Audebert et al., 1993), axonemes (Bré et al., 1994), centrioles, and basal bodies (Bobinnec et al., 1998) but is also enriched in the highly dynamic mitotic spindle (Regnard et al., 1999). Tubulins are polyglutamylated at their carboxy-terminal tails, which upon assembly of MTs become exposed on the outer surface of the tubules, where they provide binding sites for several MT-associated proteins (MAPs) and molecular motors. Accordingly, MT polyglutamylation has recently been shown to regulate the activity of ciliary dynein (Kubo et al., 2010; Suryavanshi et al., 2010) and of the MT-severing protein spastin (Lacroix et al., 2010).

The enzymes that catalyze polyglutamylation, polyglutamylases, are members of a protein family sharing a homology domain with another tubulin-modifying enzyme, tubulin tyrosine ligase (TTL; Ersfeld et al., 1993), and thus are referred to as TTL-like (TTLL) proteins (Janke et al., 2005; van Dijk et al., 2007). Initial functional studies on polyglutamylases provided first evidence that polyglutamylation plays important roles in vivo. Mice knocked out for TTLL1 polyglutamylase display abnormal beating of airway epithelial cilia leading to respiratory problems (Ikegami et al., 2010). Another polyglutamylase, TTLL6, was also shown to play a role in cilia. Depletion of this enzyme in zebrafish reduced glutamylation in the olfactory placodes resulting in defective assembly of olfactory cilia (Pathak et al., 2007). Surprisingly, also overexpression of TTLL6 enzyme, which caused abnormal elongation of glutamate chains, produced ciliary defects in *Tetrahymena* (Janke et al., 2005; Wloga et al., 2009). Taken together, this suggests that maintaining the correct levels of tubulin polyglutamylation by the coordinated action of polyglutamylases and deglutamylating enzymes is essential. The aim of the present work was to identify deglutamylating enzymes and analyze their functions in vivo.

Recent studies of a family of cytosolic carboxypeptidases (CCPs) have suggested that one of the members of this family, CCP1 (also known as Nna1), is the enzyme that removes the C-terminal tyrosine from α-tubulin (Kalinina et al., 2007; Rodriguez de la Vega et al., 2007); however convincing evidence has not been provided. The possibility that CCP1 is involved in tubulin modifications was exciting because loss of function of

CCP1 had been associated with the phenotypes observed in *Purkinje cell degeneration* (*pcd*) mice (Fernandez-Gonzalez et al., 2002). *pcd* mice display multiple defects including degeneration of several types of neurons. The first neurons to be lost are Purkinje cells, which die during early adulthood leading to ataxia. The loss of Purkinje cells is followed by degeneration of cerebellar granule neurons (CGNs), and later some populations of thalamic neurons also disappear (Mullen et al., 1976). Moreover, mitral cells from the olfactory bulb as well as retinal photoreceptors degenerate progressively over 1 year. Finally, the males are sterile and the females experience difficulties giving birth (reviewed in Wang and Morgan, 2007). Recent studies demonstrated that Purkinje cell loss as well as retinal degeneration observed in the *pcd* mice could be rescued by wild-type (WT) CCP1 but not an inactive CCP1 (Chakrabarti et al., 2008; Wang et al., 2006). This demonstrated that the lack of CCP1 carboxypeptidase activity is responsible for the phenotypes observed in the *pcd* mice; however, the molecular mechanisms underlying the numerous defects remain unclear.

Here, we show that CCP1 specifically catalyzes the removal of the penultimate glutamate residue from detyrosinated α-tubulin, thus generating Δ2-tubulin; however, it is not involved in detyrosination itself. Moreover, we demonstrate that the removal of gene-encoded glutamic acids from the C termini of proteins is not specific to tubulin but affects a range of substrates including myosin light chain kinase 1 (MLCK1). Apart from the deglutamylation of protein primary sequence, CCP1 also shortens posttranslationally generated glutamate side chains on tubulin and is therefore a tubulin deglutamylase. We further demonstrate the existence of two functional homologs of CCP1, CCP4, and CCP6, and we provide evidence that another recently described deglutamylating enzyme, CCP5 (Kimura et al., 2010), specifically removes the branching point glutamates generated by polyglutamylation. Finally, we have analyzed the neurodegeneration phenotype in the *pcd* mice in light of the newly identified deglutamylating activity of CCP1. Consistent with the enzymatic activity of CCP1, we show that tubulin polyglutamylation is highly increased specifically in brain areas that degenerate in the *pcd* mice. Moreover, by downregulating polyglutamylation, we were able to partially prevent neurodegeneration, providing direct evidence that abnormally high polyglutamylation levels lead to neuronal degeneration.

RESULTS

CCP1 Generates Δ2-Tubulin and Also Acts as a Tubulin Deglutamylase

Recent studies have suggested that CCP1 is involved in α-tubulin detyrosination (Kalinina et al., 2007). To directly test this idea, we performed immunoblot analysis of protein extracts prepared from HEK293 cells expressing either active or enzymatically inactive (dead, Figure S1 available online) murine CCP1. Although we did not observe any increase in the level of tubulin detyrosination, we detected an ectopic appearance of a related tubulin modification, Δ2-tubulin (Paturle-Lafanechere et al., 1991). Thus, CCP1 seems to catalyze the removal of the penultimate glutamate residue, but not detyrosination itself. To further test whether CCP1 is specifically generating Δ2-tubulin, we expressed this protein in mouse embryonic fibroblasts (MEFs) and stained the cells with antibodies for tyrosinated and Δ2-tubulin. There was no obvious reduction in the level of tyrosinated tubulin, but we observed a strong increase in the labeling for Δ2-tubulin specifically in cells expressing CCP1 (Figure 1B). This increase in the level of Δ2-tubulin was not observed when the enzymatically dead version of CCP1 was expressed (Figure S2A). Taken together these results demonstrate that CCP1 catalyzes the removal of the very C-terminal glutamate residue from detyrosinated α-tubulin, but it is not involved in α-tubulin detyrosination.

Considering that CCP1 was associated with α-tubulin primary sequence deglutamylation, we speculated that it might also catalyze the removal of glutamate side chains, which are added to α- and β-tubulin as a result of posttranslational polyglutamylation (Eddé et al., 1990; Rüdiger et al., 1992). To test this hypothesis, we expressed CCP1 in neurons, which are known to carry a high level of tubulin polyglutamylation (Audebert et al., 1993), and labeled them with polyE antibody that recognizes glutamate chains composed of at least three glutamic acids (Figure S3). Neurons expressing active but not inactive CCP1 showed a strong reduction in the level of polyE signal (Figure 1C and Figure S2B). These results show that CCP1 is indeed involved in the removal of posttranslational polyglutamylation.

To further characterize the deglutamylation activity of CCP1, we set up an in vitro deglutamylation assay in which highly polyglutamylated brain tubulin was incubated with protein extract from HEK293 cells expressing either active or inactive CCP1. The status of polyglutamylation was examined with two polyglutamylation-specific antibodies: polyE that recognizes long glutamate side chains, and GT335 that recognizes all glutamylated forms of tubulin because it is specific to the branching point of the glutamate side chain (Wolff et al., 1992). In combination, these two antibodies allowed us to distinguish between tubulin carrying either short or long glutamate side chains. Brain tubulin treated with active CCP1 was no longer detected by polyE antibodies, while the GT335 signal was not decreased (Figure 1D). This indicated that CCP1 shortens the glutamate side chains of brain tubulin without removing the branching point glutamates. Similar results were obtained with purified 6His-CCP1, confirming that CCP1 directly catalyzes tubulin deglutamylation (Figures S2C and S2D). To further investigate the enzymatic specificity of CCP1 for long side chains, we assayed the enzyme with mono- or polyglutamylated tubulin purified from HeLa cells after overexpression of different TTLL glutamylating enzymes (van Dijk et al., 2007). When monoglutamylated tubulin (modified by TTLL4) was incubated with active CCP1, no changes in glutamylation levels were observed, indicating that CCP1 cannot remove the short side chains generated by TTLL4 (Figure 1D). Surprisingly, when tubulin polyglutamylated with TTLL6 was incubated with CCP1, a strong reduction in both polyE and GT335 signals was observed (Figure 1D). This indicated that besides shortening the polyglutamate side chains, CCP1 also removes the branching point glutamates when the glutamylation is generated by TTLL6 but not by TTLL4 or by TTLL1, which generates most of the glutamylation present on brain MTs (Janke et al., 2005). To validate that the removal of the branching point glutamates by CCP1 depends on the

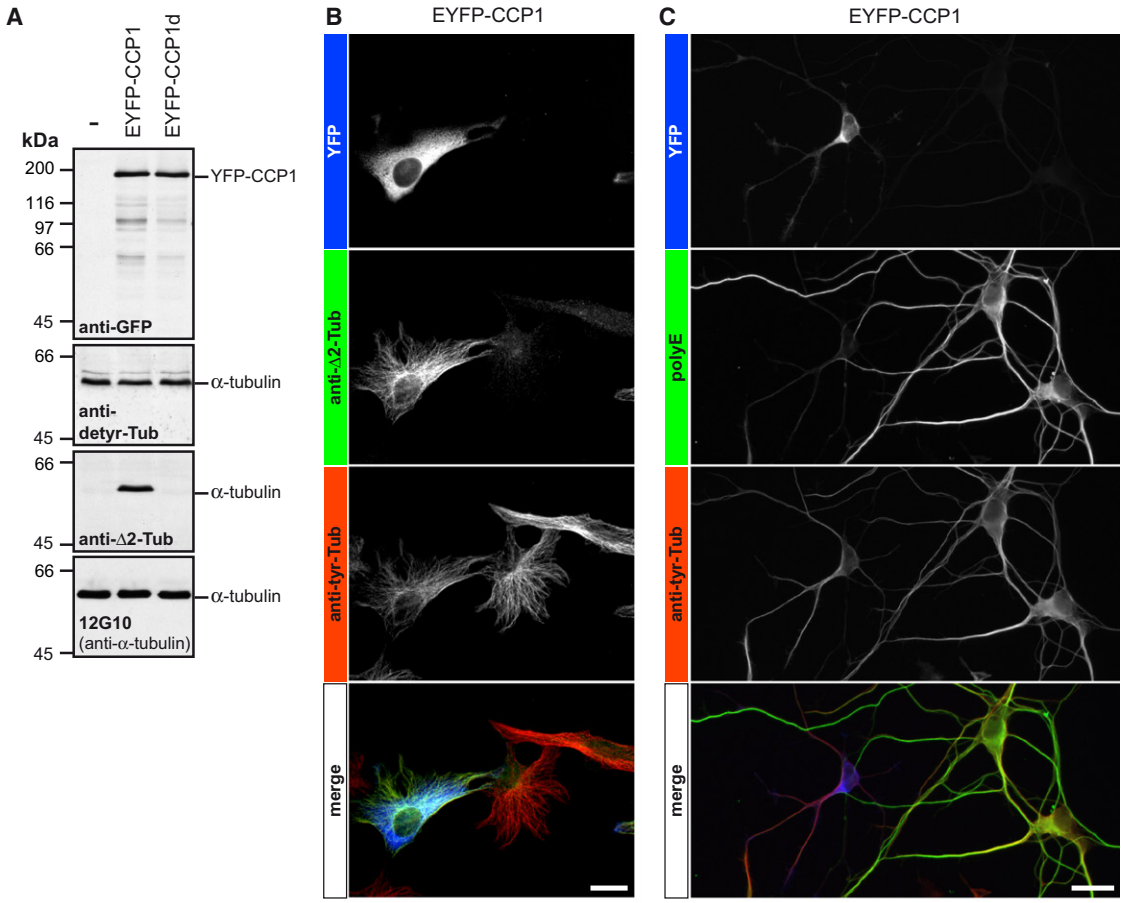
A
-
EYFP-CCP1
EYFP-CCP1d
kDa
200
116
97
66
45
YFP-CCP1
anti-GFP
66
45
α-tubulin
anti-detyr-Tub
66
45
α-tubulin
anti-Δ2-Tub
66
45
α-tubulin
12G10
(anti-α-tubulin)
B
EYFP-CCP1
YFP
anti-Δ2-Tub
anti-tyr-Tub
merge
C
EYFP-CCP1
YFP
polyE
anti-tyr-Tub
merge

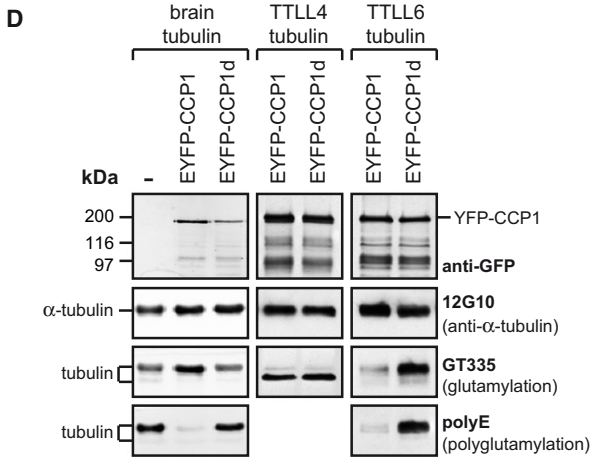
D
brain tubulin
TTLL4 tubulin
TTLL6 tubulin
EYFP-CCP1
EYFP-CCP1d
kDa
-
200
116
97
YFP-CCP1
anti-GFP
α-tubulin
12G10
(anti-α-tubulin)
tubulin
GT335
(glutamylation)
tubulin
polyE
(polyglutamylation)

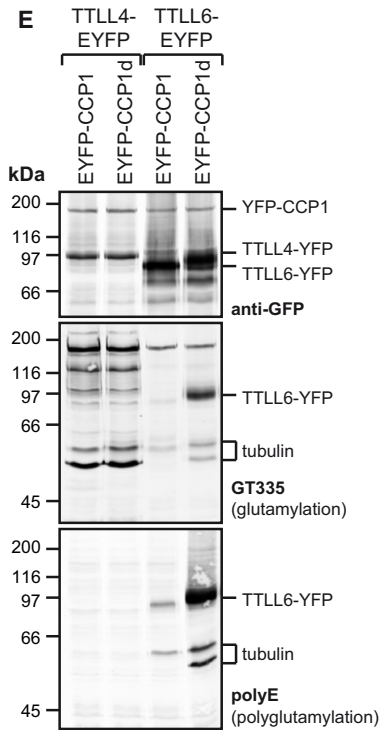
E
TTLL4-EYFP
TTLL6-EYFP
EYFP-CCP1
EYFP-CCP1d
kDa
200
116
97
66
YFP-CCP1
TTLL4-YFP
TTLL6-YFP
anti-GFP
45
TTLL6-YFP
tubulin
GT335
(glutamylation)
TTLL6-YFP
tubulin
polyE
(polyglutamylation)

enzyme that has generated glutamylation in the first place, we set up cotransfection experiments. CCP1 was coexpressed together with TTLL4 or TTLL6 in HEK293 cells, and the cell extracts were analyzed by immunoblot. In agreement with our in vitro data, expression of CCP1 had no effect on the glutamylation status of tubulin and other proteins that are modified by TTLL4. In contrast, CCP1 blocked the accumulation of both mono- and polyglutamylation on TTLL6 substrates, which include tubulins and TTLL6 itself (Figure 1E). These results confirmed that CCP1, in addition to shortening long glutamate chains, also removes the branching point glutamates when the modification is generated by TTLL6 but not TTLL4.

Tubulin Modifications in the *pcd* Mouse that Lacks Active CCP1

To study the role of CCP1 in vivo, we took advantage of *Purkinje cell degeneration* (*pcd*^{3J}) mice in which a deletion in the *CCP1* gene results in loss of function of the CCP1 protein (Fernandez-Gonzalez et al., 2002). Based on our discovery of the deglutamylating activity of CCP1 we expected the absence of Δ2-tubulin and increased tubulin polyglutamylation in the *pcd* mice. To test our predictions we compared the status of tubulin modifications between *pcd* and WT mice. Protein extracts from several organs were analyzed by immunoblot with antibodies recognizing either the unmodified C-terminal α-tubulin tail (tyrosinated tubulin) or its processed versions (detyrosinated or Δ2-tubulin), as well as with polyE antibodies specific to long glutamate chains. When comparing the levels of tyrosinated and detyrosinated tubulin between *pcd* and WT mice, we observed no differences in all organs analyzed. Surprisingly, the Δ2-tubulin modification was also unchanged in most of the organs except skeletal muscles, where we detected a strong reduction (Figure 2A). This confirmed that CCP1 is involved in generating Δ2-tubulin in vivo, but at the same time it implied the existence of additional enzyme(s) catalyzing this modification. Tubulin polyglutamylation, for which we expected an increase in the *pcd* mice, at least in the organs where tubulin glutamylases are highly expressed such as brain and testes, was indeed slightly increased relative to the equal levels of tyrosinated tubulin in these two organs (Figure 2A). These results are in agreement with CCP1 being involved in the removal of posttranslational tubulin polyglutamylation.

In contrast to mostly slight changes in the levels of tubulin posttranslational modifications observed in the *pcd* mice, we detected protein bands outside of the tubulin region that reacted with anti-Δ2-tubulin exclusively in the WT mice. Conversely, bands of corresponding size were labeled by detyrosinated or polyE antibodies in the *pcd* mice (Figure 2A). This suggested the existence of proteins that end with a -GE$_n$ sequence at their C termini, which is recognized in the *pcd* mice with polyE (if $n \geq 3$) or with detyrosinated antibody (if n = 2). However, in WT mice, both types of proteins have C termini shortened to -GE (specifically detected with anti-Δ2-tubulin antibody), most likely by the enzymatic activity of CCP1. Thus, C-terminal deglutamylation seems to be a modification that is not restricted to tubulin.

MLCK1 and Telokin Are Substrates of CCP1

Two of the potential CCP1 substrates (~130 kDa and ~20 kDa) were prominent in stomach and one (~130 kDa) in the uterus (Figure 2A). In order to identify these substrates, we prepared protein extract from mouse stomach and analyzed the two anti-Δ2-reactive bands by mass spectrometry. Several proteins were identified (Table S2 and Table S3), but only two appeared as promising candidates for being processed by CCP1. Myosin light chain kinase 1 (130 kDa MLCK1) and telokin, a 17 kDa protein corresponding to the C-terminal fragment of MLCK1 (Smith et al., 1998), end with the sequence -EGEEGGEEEEEEEE. Thus, both proteins could be detected with polyE, or when processed by CCP1 to -EGEEGGE with anti-Δ2-tubulin antibody. To provide additional evidence that MLCK1 undergoes C-terminal deglutamylation, we used an anti-MLCK antibody for immunoprecipitation from stomach and uterus extracts and showed that the immunoprecipitated protein was detected by anti-Δ2-tubulin antibodies (Figure 2B). To demonstrate that MLCK and telokin are processed by CCP1, we expressed them together with active or inactive CCP1 in HEK293 cells and analyzed the protein extracts by immunoblot (see Figure S3 for antibody specificities). In the presence of inactive CCP1, both MLCK1 and telokin were recognized by polyE but not anti-Δ2-tubulin antibodies. In contrast, when MLCK1 and telokin were expressed together with active CCP1, both proteins were labeled by anti-Δ2-tubulin but not polyE antibodies (Figure 2C). To confirm that CCP1 directly catalyzes primary sequence deglutamylation, we incubated purified GST-telokin with purified 6His-CCP1. GST-telokin treated with CCP1 was recognized by anti-Δ2-tubulin but not polyE antibodies, demonstrating that CCP1 shortened the C-terminal glutamate stretch (Figure 2D). Primary sequence deglutamylation was no longer observed in the presence of phenanthroline, a specific inhibitor of metalloproteases (Figure 2D). These results clearly show that MLCK1 and telokin are directly processed by CCP1 in the way that seven out of eight C-terminal glutamates are removed from the C termini of these proteins.

Finally, we tested whether CCP1 activity is restricted to the removal of glutamates, or if this enzyme could potentially also process other amino acids. Based on telokin, we generated several artificial substrates ending with the C-terminal sequences -GED, -GEEDD, -GEEY, and -GEEF. All of these

Figure 1. Enzymatic Characterization of CCP1

(A) Immunoblot of protein extracts from HEK293 cells expressing active (EYFP-CCP1) or inactive (EYFP-CCP1d) CCP1.

(B) Immunofluorescence of mouse embryonic fibroblasts (MEFs) expressing EGFP-CCP1. Anti-Δ2-tubulin antibody specifically labels the cell expressing EGFP-CCP1.

(C) Immunofluorescence of mouse hippocampal neurons expressing EGFP-CCP1. PolyE antibody does not label the cell expressing EGFP-CCP1.

(D) Immunoblot of tubulin treated with extracts from HEK293 cell expressing either active or inactive EYFP-CCP1. Three types of tubulin were used: brain tubulin and HeLa tubulin modified with either TTLL4 or TTLL6. TTLL4 does not generate a polyE signal on tubulin (not shown).

(E) Immunoblot of protein extracts prepared from HEK293 cells coexpressing TTLL4-EYFP or TTLL6-EYFP together with active or inactive EYFP-CCP1. Note that the GT335 signal generated by TTLL4 is not removed by CCP1, whereas TTLL6-dependent GT335 labeling on tubulin and TTLL6 is reduced by CCP1.

Scale bars in (B) and (C) are 20 μm. See also Figure S1 and Figure S2.

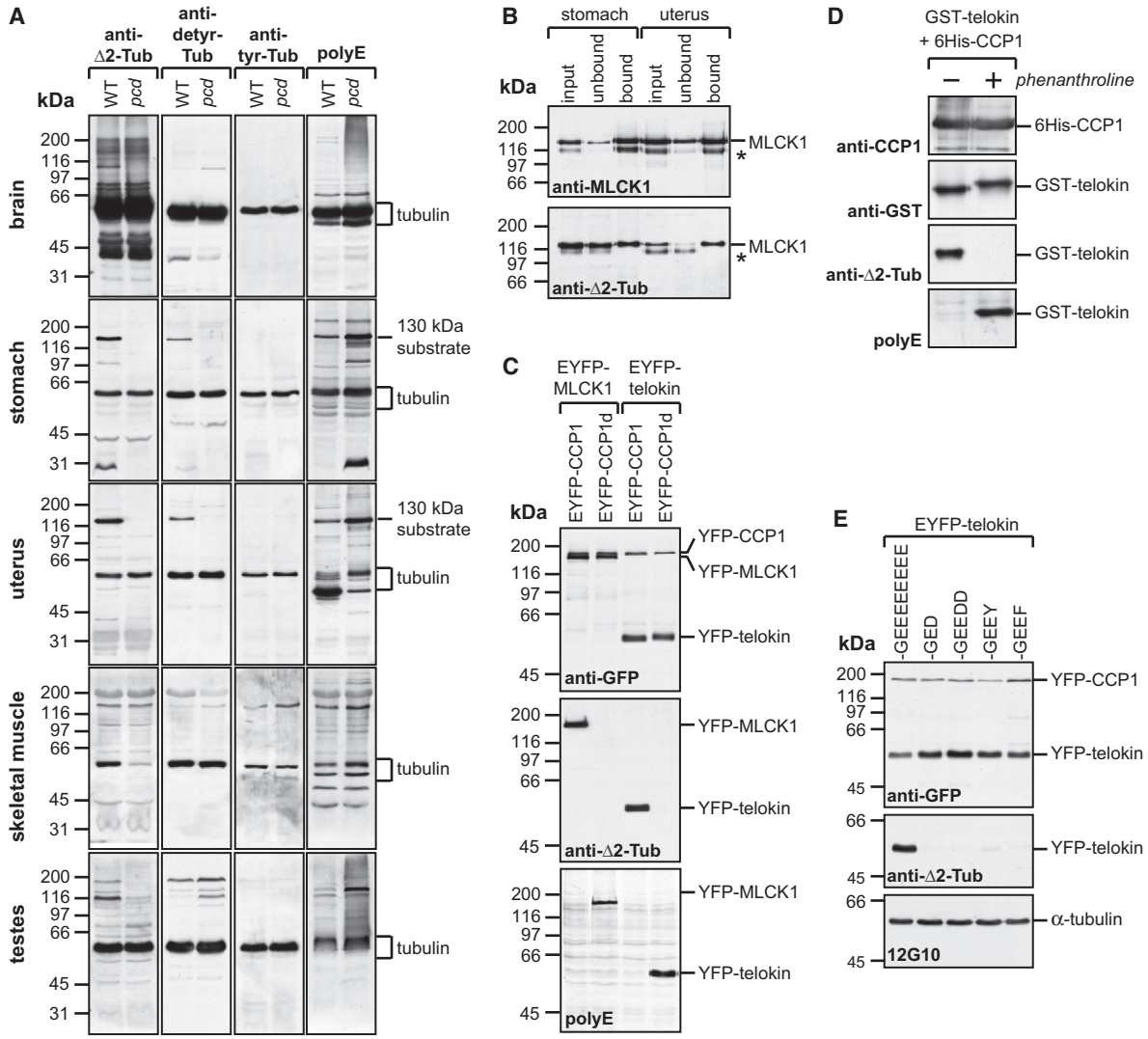

Figure 2. Characterization of CCP1 Substrates

(A) Comparative immunoblot of protein extracts prepared from organs of WT and *pcd* mice. Whole-tissue extracts were tested with anti-tyr-tubulin, detyr-tubulin, Δ2-tubulin, and polyE. Note the disappearance of anti-Δ2-tubulin and anti-detyr-tubulin labeling and increase in polyE staining for 130 kDa substrate in the extracts from stomach and uterus of the *pcd* mice.

(B) Immunoprecipitations with anti-MLCK1 antibodies using protein extracts from stomach and uterus of WT mice. The fractions were tested in immunoblot. In the bound fraction, protein bands of the same size are detected with anti-Δ2-tubulin and anti-MLCK1 antibodies. (*degradation product.)

(C) Immunoblot of protein extracts prepared from HEK293 cells coexpressing EYFP-CCP1 or EYFP-CCP1d together with EYFP-MLCK1 or EYFP-telokin. The Δ2-tubulin labeling correlates with the expression of active CCP1, and polyE labeling correlates with the expression of inactive CCP1.

(D) In vitro deglutamylation assay with purified GST-telokin and 6His-CCP1. GST-telokin and 6His-CCP1 were incubated in the presence or absence of phenanthroline. GST-telokin is specifically detected with Δ2-tubulin antibody after incubation with 6His-CCP1. In the presence of phenanthroline, telokin remains in the polyE-reactive form and is not detected by anti-Δ2-tubulin antibody.

(E) Immunoblot of protein extract from HEK293 cells coexpressing EYFP-CCP1 and different artificial substrates based on EYFP-telokin. The sequence of the C-terminal tails of the telokin-like substrates is indicated starting from glycine 151. Only WT telokin (-GEEEEEEEE) coexpressed with CCP1 is labeled by anti-Δ2-tubulin antibody.

See also Figure S3, Table S1, Table S2, Table S3, and Table S4.

artificial telokins including WT telokin were cotransfected with CCP1 in HEK293 cells, and the protein extracts were analyzed with anti-Δ2-tubulin antibodies on immunoblot. Only WT telokin was detected with anti-Δ2-tubulin antibody (Figure 2E), indicating that CCP1 is a highly specific carboxypeptidase that exclusively cuts peptide bonds between two C-terminally located glutamates. Even aspartate, the amino acid that most closely resembles glutamate, was not removed by CCP1. In addition, aromatic residues such as tyrosine and phenylalanine were also blocking deglutamylation of telokin, which is coherent with our data indicating that CCP1 does not catalyze α-tubulin detyrosination.

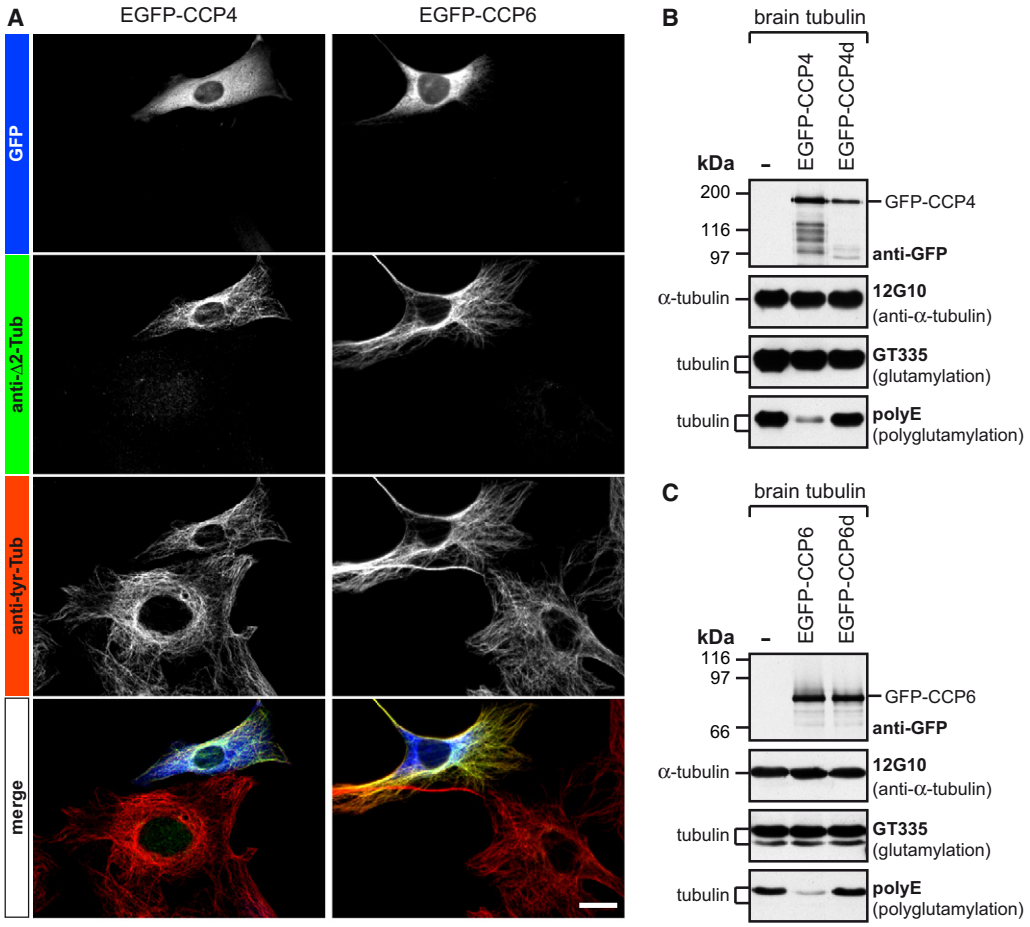

Figure 3. Enzymatic Characterization of CCP4 and CCP6

(A) Immunofluorescence of MEFs expressing either EGFP-CCP4 or EGFP-CCP6. Scale bar is 20 μm.

(B and C) Immunoblot of brain tubulin treated with protein extracts from HEK293 cells expressing (B) active or inactive EGFP-CCP4 and (C) active or inactive EGFP-CCP6. Note the specific reduction of polyE signal after the treatment with active CCP4 or CCP6.

See also Figure S1 and Figure S4.

CCP4 and CCP6 Also Generate Δ2-Tubulin and Act as Long-Chain Deglutamylases

Our observation that in most of the organs of the *pcd* mice, except skeletal muscles, Δ2-tubulin levels are comparable to those in WT mice (Figure 2A) clearly showed that additional enzyme(s) are involved in Δ2-tubulin generation. The CCP protein family, apart from CCP1, contains five additional members (Kalinina et al., 2007; Rodriguez de la Vega et al., 2007). To test whether any of the other CCPs generates Δ2-tubulin, we expressed them in MEFs. Immunofluorescence analysis with anti-tyrosinated and anti-Δ2-tubulin antibodies demonstrated that in addition to CCP1, CCP4 and CCP6 also generate Δ2-tubulin (Figure 3A and Figure S4A). This result was confirmed by immunoblot analysis of HEK293 cells transfected with CCP4 and CCP6 (Figures S4B and S4C). The level of tyrosinated tubulin in cells expressing CCP4 and CCP6 remained unchanged, indicating that these enzymes, similarly to CCP1, do not detyrosinate tubulin (Figure 3A). We further tested whether CCP4 and CCP6 also remove polyglutamylation. Using in vitro deglutamylation assays with brain tubulin and protein extracts from HEK293 cells expressing either CCP4 or CCP6, we observed a strong reduction in the polyE but not GT335 signal (Figures 3B and 3C). Finally, we tested whether CCP4 and CCP6 also remove glutamates from the primary sequence of MLCK1 and telokin. After coexpressing MLCK or telokin with CCP4 or CCP6 in HEK293 cells, both substrates were labeled with anti-Δ2-tubulin but not polyE antibodies (Figures S4D and S4E). Thus CCP4 and CCP6 generate Δ2-tubulin, catalyze shortening of glutamate side chains, and remove all but one of the C-terminal glutamates from MLCK1 and telokin, indicating that they are functional homologs of CCP1.

Progressive Accumulation of Polyglutamylation in the Cerebellum and Olfactory Bulb of the *pcd* Mice

Our immunoblot analysis of tubulin posttranslational modifications demonstrated that tubulin polyglutamylation is slightly increased in the brain of adult *pcd* mice (Figure 2A). To test whether this increase was confined to regions where

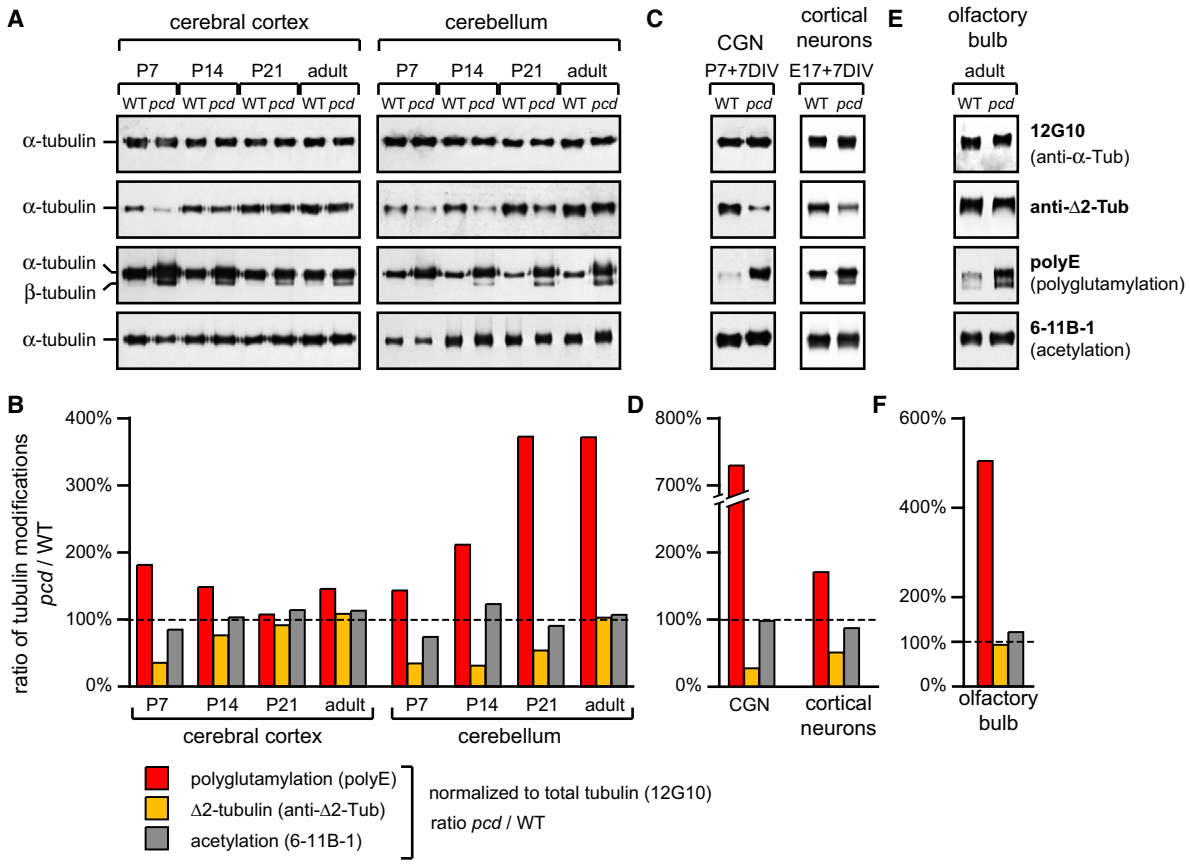

Figure 4. Analysis of Tubulin Modifications in Different Brain Regions of the *pcd* Mice

(A) Immunoblot of protein extracts prepared from the cerebellum and cerebral cortex of WT and *pcd* mice at different stages of brain development (postnatal days [P] 7, 14, and 21 and adult animals).

(B) Graphical representation of antibody signals detected in (A). The plotted values represent the relative intensities of the immunoblots of *pcd* samples (WT = 100%) after normalization to total tubulin levels (12G10).

(C) Immunoblot of protein extracts from cerebellar granule neurons (CGNs) isolated at postnatal day 7 (P7) or cortical neurons isolated at embryonic day 17 (E17) and cultured for 7 days (7DIV).

(D) Graphical representation of modification levels in *pcd* versus WT neurons. Relative intensities were calculated as in (B).

(E) Immunoblot of protein extracts from the olfactory bulbs of adult mice.

(F) Graphical representation of modification levels in *pcd* versus WT samples. Relative intensities were calculated as in (B).

See also Figure S5.

neurodegeneration occurred, we analyzed the status of tubulin modifications in the cerebellum, a part of the brain with extensive degeneration, and in cerebral cortex where no degeneration has been observed. Protein extracts from P7, P14, P21, or adult WT and *pcd* mice were analyzed by immunoblot with antibodies specific to tubulin modifications. At early developmental stages, Δ2-tubulin levels were strongly reduced in both the cerebellum and cortex of the *pcd* mice as compared to WT (Figures 4A and 4B; lanes "P7"; Figure S5A). At later stages, Δ2-tubulin gradually increased reaching WT levels in adult mice. However, the restoration of Δ2-tubulin modification occurred earlier in the cortex as compared to the cerebellum (Figures 4A and 4B).

Consistent with the deglutamylation activity of CCP1, the degree of tubulin polyglutamylation was strongly increased in the cortex and cerebellum of young *pcd* mice (Figures 4A and 4B; lanes "P7"; Figure S5A). At later stages of development, polyglutamylation in the cortex was progressively reduced to WT levels, whereas it continued to increase in the cerebellum of the *pcd* mice. Moreover, the tubulin from the cerebellum of adult *pcd* mice migrated slightly slower on the protein gel, which emphasizes the strong accumulation of long polyglutamate chains on tubulin (Figures 4A and 4B; lanes "adult"). An unrelated tubulin modification, acetylation, was not significantly affected in *pcd* mice at all developmental stages (Figures 4A and 4B). This shows that not all tubulin modifications are changed in the *pcd* mice, and that the changes observed for Δ2-tubulin and polyglutamylation are likely to be a direct result of the lack of CCP1 deglutamylating activity.

It was striking that polyglutamylation, which is strongly increased in both the cerebellum and the cortex of the *pcd* mice at earlier developmental stages, returns to WT levels in adult mice only in the cortex but not in the cerebellum (Figures 4A and 4B). This implies the existence of a compensation

mechanism that would operate in the cortex but would be inefficient in the cerebellum. A compensating mechanism for CCP1 is likely to involve enzymes with similar reaction specificities, such as CCP4 and CCP6. In situ hybridization studies have previously shown that CCP1 is highly expressed in the cerebellum and cortex of adult mouse brain, whereas CCP6 expression was rather restricted to the cortex, and CCP4 appeared to be generally expressed at low levels (Kalinina et al., 2007). We compared the expression levels of CCP1, CCP4, and CCP6 in the cortex and cerebellum at different developmental stages by reverse transcription polymerase chain reaction (Figure S5B). Whereas CCP1 appeared to be expressed at similar levels in both the cerebellum and the cortex throughout all developmental stages, CCP6 expression was very low in cerebellum as compared to cortex. CCP4 expression was generally much lower in comparison to CCP1 and CCP6 (visible only after 35 PCR cycles versus 25 cycles for CCP1 and CCP6; Figure S5B). Thus, it is possible that CCP6 compensates for the absence of CCP1 in the cortex of the *pcd* mice, whereas it is present at too low levels to achieve a complete compensation in the cerebellum. As a consequence, unopposed polyglutamylase activity results in tubulin hyperglutamylation in the cerebellum. Strikingly, Δ2-tubulin generation, which is also catalyzed by CCP1, is compensated in the cerebellum of the *pcd* mice, although less efficiently than in the cortex (Figures 4A and 4B). This might be best explained by the fact that Δ2-tubulin generation is irreversible (Paturle-Lafanechere et al., 1991), thus allowing for progressive accumulation of this modification.

To test whether the observed changes in tubulin modifications are directly related to neurons, we analyzed different types of neuronal cell cultures prepared from *pcd* and WT mice by immunoblot. Cerebellar granule neurons (CGNs) isolated from *pcd* mice at P7 and cultured for 7 days showed increased levels of polyglutamylation and decreased Δ2-tubulin as compared to CGNs isolated from WT mice, whereas tubulin acetylation was unchanged. Similar results were obtained for primary cultures of cortical neurons isolated from WT and *pcd* mice at embryonic day (E) 17 and cultured for 7 days (Figures 4C and 4D). Since both neuronal cultures contained only very low amounts of glia cells, these findings strongly suggest that the changes in tubulin modifications observed in the extracts of the cerebellum and cortex of *pcd* mice are related to neurons.

The correlation between tubulin hyperglutamylation and neurodegeneration in the cerebellum of adult *pcd* mice suggested that degeneration of other regions of the brain in these mice might also be related to increased tubulin polyglutamylation. To test this hypothesis, we analyzed the status of tubulin modifications in the olfactory bulbs, known to undergo neurodegeneration in adult *pcd* mice. Similarly to cerebellum, we observed strong increase in the levels of tubulin polyglutamylation, whereas acetylation and Δ2-tubulin levels were unchanged (Figures 4E and 4F). Thus, our results suggested that neurodegeneration observed in the *pcd* mice is related to hyperglutamylation.

Purkinje Cell Degeneration in *pcd* Mice Is Caused by Tubulin Hyperglutamylation

To unambiguously demonstrate the causal link between hyperglutamylation of tubulin observed in the *pcd* mice and neurodegeneration, we aimed to rescue the Purkinje cell degeneration by reducing the polyglutamylation levels in these neurons. Based on the observation that most of the tubulin polyglutamylase activity in brain is associated with the TTLL1-polyglutamylase complex (Janke et al., 2005), we used shRNA that specifically depletes TTLL1 to reduce polyglutamylation levels (Figure S6). Lentivirus expressing TTLL1-specific shRNA (shTTLL1) and GFP or control virus expressing only GFP were injected in the cerebellum of 10-day-old (postnatal day [P] 10) WT or *pcd* mice. The mice were analyzed 30 days after injection (P40) by behavioral tests and immunohistochemistry.

Analysis of cerebella from WT mice injected with control virus (n = 6) showed that the differentiation of the Purkinje cell layer was not affected by the virus injections, and that some of the fully developed Purkinje cells expressed GFP, indicating that these cells were infected by the virus (Figures 5A and 5B, panels "WT + control virus"). Cerebella from *pcd* mice injected with control virus (n = 5) showed a complete degeneration of the Purkinje cell layer 30 days post-injection, which is in accordance with the expected degeneration of *pcd* mice cerebella at this age (Figure 5A, panels "*pcd* + control virus"). In contrast, *pcd* mice cerebella injected with shTTLL1 virus (n = 6) displayed a large number of morphologically normal Purkinje cells in the injected (GFP-positive) regions of the brain, which was not the case in noninjected areas (Figures 5A and 5B, panels "*pcd* + virus shTTLL1"). The rescue of Purkinje cell degeneration by the downregulation of TTLL1 polyglutamylase demonstrates that unopposed posttranslational polyglutamylation is the primary cause of the neuronal degeneration in the *pcd* mice.

To determine whether mice injected with shTTLL1 virus have improved their motor coordination, we performed rotarod tests. Under our experimental conditions, *pcd* mice injected with control virus fell off the rod after ~12 s whereas *pcd* mice injected with shTTLL1 virus remained on the rod for ~22 s (Figure 5C). Thus, injection of shTTLL1 virus in the cerebellum of *pcd* mice led to a significant improvement of the motor coordination of these mice.

CCP5 Is a Protein Deglutamylase that Specifically Removes the Branching Point Glutamates

Based on the analysis of CCP1, CCP4, and CCP6, it became obvious that none of these enzymes catalyzed the removal of branching point glutamates generated by TTLL4, or the ones present on mouse brain MTs. To identify the enzyme(s) responsible for the removal of these branching points, we screened the remaining CCP family members for such activity by coexpressing them with TTLL4. Using immunofluorescence, we identified CCP5 as the only enzyme that was able to remove TTLL4-dependent monoglutamylation in U2OS cells. This process was activity dependent, as an inactive version of CCP5 did not prevent TTLL4-mediated glutamylation of MTs (Figure 6A). To further characterize the specificity of CCP5, we used immunoblots with GT335 and polyE antibodies to compare the glutamylation levels in HEK293 cells coexpressing CCP5 with either TTLL4 or TTLL6. Whereas coexpression of TTLL4 with inactive CCP5 induced monoglutamylation on several proteins, including α- and β-tubulin, the coexpression with active CCP5 completely

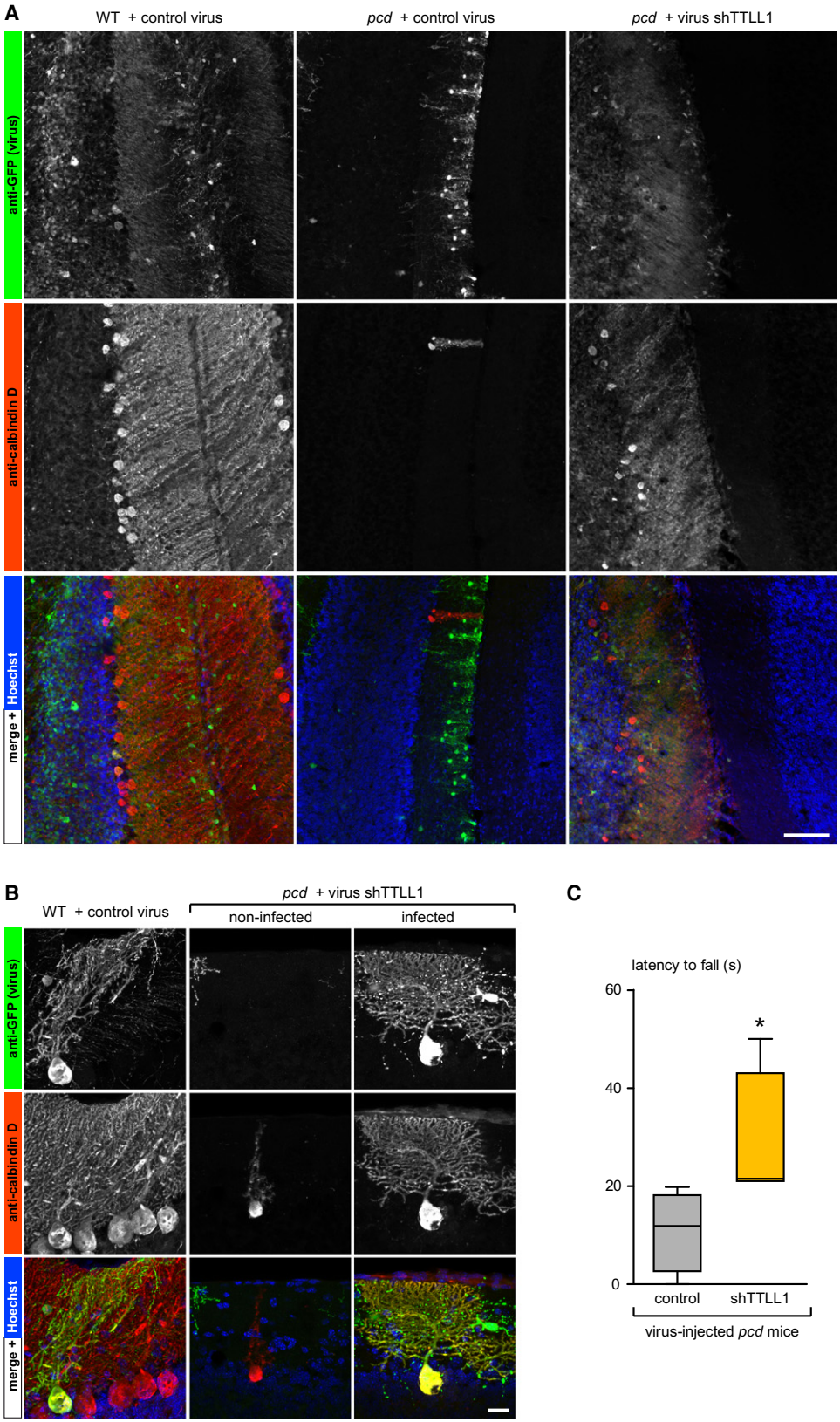
A
WT + control virus
pcd + control virus
pcd + virus shTTLL1
anti-GFP (virus)
anti-calbindin D
merge + Hoechst
B
WT + control virus
pcd + virus shTTLL1
non-infected
infected
anti-GFP (virus)
anti-calbindin D
merge + Hoechst
C
latency to fall (s)
60
40
20
0
*
control
shTTLL1
virus-injected pcd mice

blocked the modification of the TTLL4 substrates (Figure 6B). This suggested that CCP5 removes glutamylation not only from tubulin but also from other substrates that were monoglutamylated by TTLL4. In the case of TTLL6, expression with inactive CCP5 resulted in generation of GT335 and polyE signals on tubulins and TTLL6 itself, whereas expression with active CCP5 completely removed monoglutamylation and strongly reduced polyglutamylation of tubulin. In addition, active CCP5 induced a slight reduction of the GT335 labeling of the TTLL6 protein band whereas the polyE signal remained unchanged, indicating that only short side chains are removed (Figure 6B). Taken together, these results clearly show that CCP5 removes branching point glutamates regardless of whether they were generated by TTLL4 or TTLL6.

To determine whether the reduction in polyE signal after coexpressing TTLL6 with CCP5 is related to a long chain deglutamylase activity of CCP5, or if it was indirectly caused by the removal of short side chains prior to elongation, we tested CCP5 in an in vitro deglutamylation assay with brain tubulin. Brain MTs are known to carry mostly long glutamate chains on α-tubulin, whereas side chains on β-tubulin are predominantly short (Redeker et al., 2004). When brain tubulin was incubated with active CCP5, we observed complete removal of GT335 signal from β-tubulin but only a slight reduction of the signal on α-tubulin. In contrast, no changes in the polyE signal were observed (Figure 6C). These results strongly suggest that CCP5 activity is restricted to the removal of branching point glutamates, and that the enzyme does not shorten or remove long glutamate chains. To confirm this hypothesis, we performed additional in vitro assays using tubulin purified from HeLa cells overexpressing TTLL4 (tubulin with short glutamate chains) or TTLL6 (tubulin with long glutamate chains). Although CCP5 completely removed GT335 signal from TTLL4-modifed tubulin, it only slightly reduced the GT335 labeling on TTLL6-modified tubulin and did not affect the polyE labeling. Together with the observation that CCP5 does not generate Δ2-tubulin (not shown), these data are in agreement with CCP5 being a deglutamylase that specifically removes branching point glutamates (Figure 6C).

Cooperative Mechanism of Tubulin Deglutamylation

To test whether the enzymes associated with each step of the deglutamylation reaction could cooperate in the complete elimination of polyglutamate chains, we performed an in vitro deglutamylation assay in which we combined enzymes that shorten long glutamate chains (CCP1, CCP4, and CCP6) with CCP5 that removes branching point glutamates. As a control we also treated brain tubulin with each of the enzymes separately. In agreement with our previous observations, CCP1, CCP4, and CCP6 strongly reduced poly- but not monoglutamylation on brain tubulin, whereas CCP5 treatment resulted in a slight reduction of mono- but not polyglutamylation. However, when we treated brain tubulin with a mixture of CCP5 and either CCP1, CCP4, or CCP6, the polyglutamylation was completely eliminated and monoglutamylation was decreased to almost undetectable levels (Figure 6D). These results clearly show that the two types of deglutamylating enzymes act in a cooperative manner and that tubulin polyglutamylation is a completely reversible posttranslational modification.

DISCUSSION

A Family of Enzymes Catalyzing the Removal of Posttranslational Polyglutamylation

Since the discovery that polyglutamylation is a strictly regulated posttranslational modification (Audebert et al., 1993), the identification of the enzymes involved in generation and removal of the glutamate side chains was considered as the key step toward systematic functional studies. Whereas the glutamylating enzymes have been identified (Janke et al., 2005; van Dijk et al., 2007), the reverse enzymes have remained unknown until the very recent description of a first mammalian deglutamylase, CCP5 (Kimura et al., 2010). Here we provide evidence that in mammals, besides CCP5, three additional members of the CCP family (CCP1, CCP4, and CCP6) catalyze protein deglutamylation. We further show that the CCP deglutamylases differ in their enzymatic specificities. On highly polyglutamylated brain tubulin, CCP1, CCP4, and CCP6 catalyze the shortening of the glutamate side chains, while CCP5 exclusively removes the branching point glutamates (schematic representation: Figure 7). A mechanism in which two types of enzymes cooperate to completely remove polyglutamylation on brain MTs is in agreement with the previous observation that deglutamylation in neurons occurs at two different rates: a fast rate for shortening of long glutamate side chains and a slower rate for the removal of branching point glutamates (Audebert et al., 1993). This differential deglutamylation might allow for a tight control over the distribution of mono- and polyglutamylation on MTs within cells or even along single MTs.

Figure 5. Rescue of Purkinje Cell Degeneration by TTLL1 Depletion

(A) Immunohistochemistry of thin cerebellar sections of WT or *pcd* mice injected with lentivirus expressing either GFP (control) or GFP and shTTLL1 (Figure S6). Purkinje cells are visualized with anti-calbindin D antibody, and the GFP signal was amplified using an anti-GFP antibody. In the panels that represent the *pcd* cerebella, only the left-hand sides of the lobes were infected by the virus (GFP). In control-injected *pcd* brains, Purkinje cells are mostly absent, whereas in shTTLL1-infected *pcd* brains, Purkinje cells survive. Note that GFP expression in Purkinje cells is clearly visible only at higher magnification (see panel B). Scale bar is 100 μm.

(B) Morphology of Purkinje cells from cerebella treated as in (A). Purkinje cells from WT brains infected with control virus show a typical highly complex dendritic tree. Note that only few Purkinje cells are infected (GFP-positive). In *pcd* mice, Purkinje cells survive rarely and show abnormal morphology (panel "non-infected"). In contrast, *pcd* Purkinje cells infected with shTTLL1 virus survived and showed normal morphology. Scale bar is 20 μm.

(C) Rotarod behavioral test of control and shTTLL1 virus-injected *pcd* mice at P40 (30 days after virus injection). The graphics represent median values with 25th–75th percentiles boxes and whiskers corresponding to the minimal and maximal values. shTTLL1-injected *pcd* mice remained significantly longer on the rotating cylinder than control-injected mice (*$p < 0.05$; Mann and Whitney, nonparametric t test, $n = 4$).

See also Figure S6.

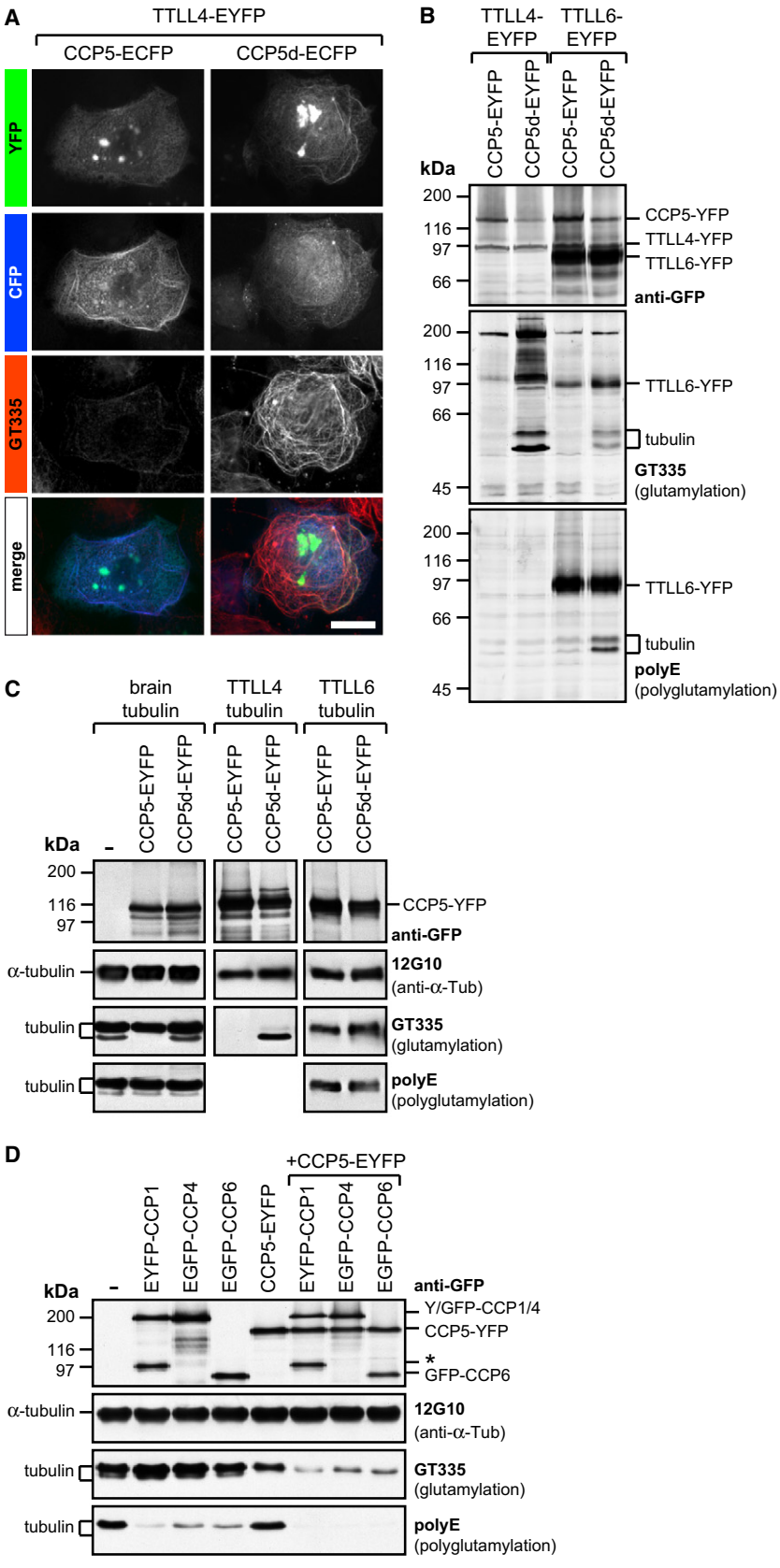

Figure 6. Enzymatic Characterization of CCP5 and the Two-Step Deglutamylation Mechanism

(A) Immunofluorescence of U2OS cells coexpressing TTLL4-EYFP and either active or inactive CCP5-ECFP. The TTLL4-dependent GT335 labeling of MTs is completely blocked by coexpression with active CCP5.

(B) Immunoblot of protein extracts from HEK293 cells coexpressing TTLL4-EYFP or TTLL6-EYFP with active or inactive CCP5-EYFP. No GT335 signal is detected after coexpression of active CCP5 and TTLL4. The GT335 and the polyE signal are strongly diminished on tubulin after coexpression of TTLL6 and active CCP5, whereas the polyE signal on TTLL6 remains unchanged.

(C) Immunoblot of tubulin treated with HEK293 cell extracts after expression of either active or inactive EYFP-CCP5. Three types of tubulin were used: brain tubulin and HeLa tubulin modified with TTLL4 or TTLL6. TTLL4-modified tubulin is not labeled with polyE (not shown).

(D) Immunoblot of brain tubulin treated with cell extracts containing each of the four CCPs or combinations of CCP5-EYFP with EYFP-CCP1, EGFP-CCP4, or EGFP-CCP6. Combinations of CCP5 and side-chain shortening enzymes leads to the removal of both polyE and GT335 signal from brain tubulin. (*degradation product of EYFP-CCP1.)

See also Figure S1.

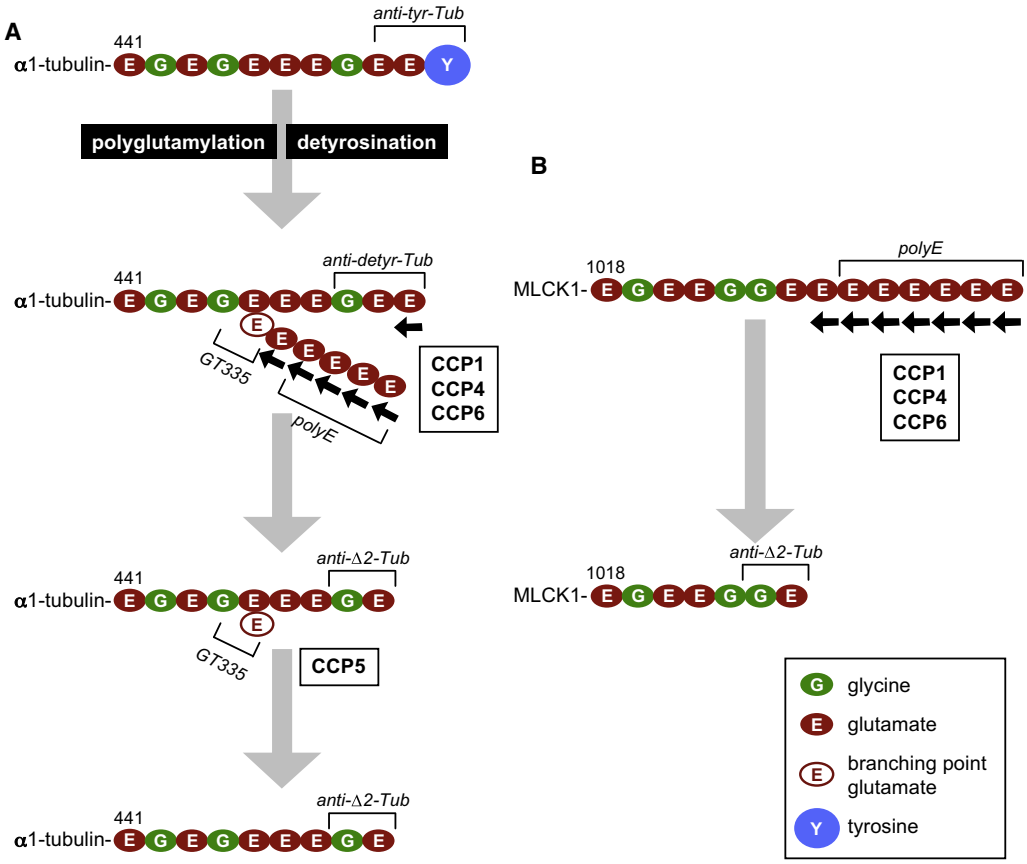

Figure 7. The Enzymatic Mechanism of Protein Deglutamylation

Schematic representation of the deglutamylation reactions catalyzed by CCP1, CCP4, CCP5, and CCP6 on brain tubulin (A) and MLCK (B; the C-terminal sequences of murine α1-tubulin and MLCK1 are represented). (A) CCP1, CCP4, and CCP6 shorten the long glutamate chains generated by posttranslational polyglutamylation, and subsequently, CCP5 removes the branching point glutamate. They also catalyze the formation of Δ2-tubulin, which requires prior detyrosination. (B) The C-terminal stretch of glutamate residues of MLCK1 is shortened to one glutamate by CCP1, CCP4, or CCP6. (A and B) The epitopes recognized by modification-specific antibodies are indicated (*italic*).

Whereas polyglutamylation on brain MTs is mainly generated by the TTLL1 polyglutamylase (Janke et al., 2005), other TTLLs are responsible for polyglutamylation of other MT types. For example, TTLL6 generates long side chains on axonemal MTs and plays an essential role in ciliary functions (Pathak et al., 2007; Suryavanshi et al., 2010; van Dijk et al., 2007). Strikingly, we found that CCP1 catalyzes complete removal of glutamate side chains including the branching point glutamates from MTs modified by TTLL6. As TTLL1 and TTLL6 both preferentially modify α-tubulin (Janke et al., 2005; van Dijk et al., 2007), this suggests that TTLL6 might utilize sites on α-tubulin that are more accessible to CCP1 than the sites modified by TTLL1. Thus, the use of different modification sites could be an additional parameter that regulates the dynamics of polyglutamylation and contributes to the diversity of signals generated by this modification.

CCPs Also Catalyze Primary Sequence Deglutamylation

Apart from posttranslationally added glutamates, CCP1, CCP4, and CCP6 also remove gene-encoded glutamates from the C termini of proteins. We have shown that these enzymes catalyze the removal of the C-terminal glutamate from detyrosinated tubulin, which gives rise to Δ2-tubulin. This form of tubulin has previously been identified as a fraction of tubulin that cannot be re-tyrosinated by TTL and that accumulates on stable MT assemblies such as neuronal MTs (Paturle-Lafanechere et al., 1994). In addition, we demonstrate that CCP1, CCP4, and CCP6 shorten the C-terminal glutamate stretch of two important regulators of myosin functions, MLCK and telokin (Gao et al., 2001; Herring et al., 2006). Out of the eight gene-encoded glutamic acids present at the very C termini of these proteins, seven are removed (Figure 7). This is in agreement with previous studies, which have revealed that telokin isolated from chicken gizzard has a variable number of glutamates at its C terminus (Rusconi et al., 1997).

Our observation that additional, not yet identified proteins undergo primary sequence deglutamylation suggests that this modification might be a general feature of proteins with multiple glutamate residues at their C termini. Understanding the functional importance of C-terminal protein deglutamylation opens an exciting new field for future research.

Polyglutamylation Is Linked to Neurodegeneration

Purkinje cell degeneration (*pcd*) mice were first described in 1976 (Mullen et al., 1976) and have since provided an excellent model to study neurodegeneration. Since the discovery that these mice lack functional CCP1 (also known as Nna1; Fernandez-Gonzalez et al., 2002), several mechanisms explaining the neurodegenerative phenotype of these mice have been proposed including lack of tubulin detyrosination, decreased protein turnover, and mitochondrial defects (Berezniuk et al., 2010; Chakrabarti et al., 2010; Kalinina et al., 2007). Based on our discovery that CCP1 is a protein deglutamylase, we have demonstrated that *pcd* mice have increased levels of tubulin polyglutamylation specifically in the parts of the brain that undergo neurodegeneration, such as the cerebellum and olfactory bulb. This suggested that tubulin hyperglutamylation could be the cause of neurodegeneration in the *pcd* mice, and indeed, downregulation of the tubulin-specific neuronal polyglutamylase (TTLL1) in the cerebellum of young *pcd* mice prevented Purkinje cell death and improved motor coordination. These experiments now unambiguously demonstrate that tubulin hyperglutamylation is responsible for the Purkinje cell degeneration in the *pcd* mice.

Tubulin polyglutamylation has been proposed to regulate a number of MT functions. Recent studies have shown that polyglutamylation regulates MT-dynein interactions (Kubo et al., 2010; Suryavanshi et al., 2010) as well as spastin-mediated MT severing (Lacroix et al., 2010). Thus, it appears that tubulin hyperglutamylation could affect the interactions of MAPs and motors with the MT cytoskeleton and as a consequence lead to neurodegeneration.

Conclusion

Here we demonstrate that unlike previously suggested, CCP1 is not the long-searched-for tubulin-detyrosinating enzyme but is involved in the removal of glutamates from tubulin as well as from other substrates. By analyzing additional members of the CCP family, we have identified a group of tubulin-modifying enzymes that generate Δ2-tubulin and that remove posttranslationally added polyglutamylation. We have also shown that the C-terminal deglutamylation of proteins is likely to be a general posttranslational modification, which might have many yet undiscovered roles in the regulation of protein functions. In addition, we found that loss of function of one of the deglutamylases in the *pcd* mice leads to MT hyperglutamylation specifically in brain regions that undergo neuronal degeneration. By depleting the tubulin-specific neuronal polyglutamylase TTLL1, we were able to prevent this degeneration, thus demonstrating that MT hyperglutamylation is the primary cause of neurodegeneration in the *pcd* mice. Taken together, we have characterized a family of deglutamylating enzymes and, by analyzing the in vivo function of one of these deglutamylases, provided evidence that the fine-tuning of the length of polyglutamate side chains on MTs is critical for neuronal function and survival.

EXPERIMENTAL PROCEDURES

Characterization of CCPs

MLCK, telokin, and CCP cDNA sequences from the NCBI database or predicted for CCP4 and CCP6 were cloned into various expression plasmids after amplification from murine cDNA. Enzymatically inactive CCPs were generated by mutagenizing a conserved zinc-binding motif (Figure S1). CCPs fused to fluorescent proteins were expressed in cultured cells. GST-tagged MLCK and telokin were expressed in bacteria, 6His-tagged CCP1 in the baculovirus-infected insect cells, and proteins were purified by affinity. Pig brain tubulin was purified as described before (Vallee, 1986). Glutamylated tubulin was purified from HeLa cells 24 hr after transfection with either TTLL4 or TTLL6 by affinity on a GT335-column as previously described (van Dijk et al., 2008). Enzymatic activities were determined by incubating the extracts of CCP-expressing HEK293 cells with brain tubulin, tubulin from HeLa cells, or purified MLCK or telokin at 37°C for 6 hr and analyzing them by SDS-PAGE and immunoblot. For immunoprecipitation, tissue extracts were incubated with protein G-coupled magnetic beads coated with anti-MLCK1 antibody, and bound proteins were analyzed by immunoblot.

Mouse Experiments

Mouse experiments were performed in accordance with institutional and national regulations and have been approved by the local ethics committee. *Pcd* mice (BALB/cByJ-*Agtpbp1*$^{pcd\text{-}3J}$-J) were obtained from The Jackson Laboratories. For tissue preparation or cell culture, mice were sacrificed and organs were quickly dissected. Control or TTLL1-specific shRNA in lentivirus was injected into the left hemisphere of the cerebellum of anesthetized P10 mouse pups using a micro-pump. Mice were analyzed 30 days after injection (P40) using behavioral tests or immunohistochemistry. Sensorimotor coordination was assayed on a rotarod. Mice were trained on the rotating cylinders at constant speed (4 rpm) until they remained on the rod for 15 s, and the latency to fall from the rod was determined by accelerating the rod every 8 s by 1 rpm. Each mouse was assayed in six successive trials, and medians were calculated and tested using the Mann and Whitney, nonparametric t test.

Cell Culture, Immunohistochemistry, and Immunoblot

Cerebellar granule neuron cultures were prepared from 7-day-old murine pups, cortical neuron cultures from E17.5 embryos, and MEFs from E13.5 embryos following standard procedures. HEK293 and HeLa cell lines were grown under standard conditions. Cells were either directly analyzed by SDS-PAGE or fixed for immunohistochemistry using standard procedures. Brain sections were permeabilized for 45 min in PBS containing 0.3% (v/v) Triton X-100 and 5% (v/v) normal goat serum (NGS), washed, and incubated overnight with primary antibody. SDS-PAGE and immunoblot were performed using standard protocols. Cells, brain sections, or membranes were incubated with rabbit polyE, anti-GFP, anti-GST, anti-detyrosinated tubulin or anti-Δ2-tubulin antibodies, mouse anti-calbindin D-28K, anti-MLCK1, GT335, 6-11B-1, and 12G10, or rat anti-tyrosinated tubulin (YL1/2) antibodies. For immunohistochemistry, anti-mouse, anti-rabbit, or anti-rat antibodies conjugated with either Alexa 555 or Alexa 488, Cy3 or Cy5 fluorophores were used and nuclei were stained using either DAPI or Hoechst 33258. Fluorescent images were acquired with a LSM 710 confocal, Axioskop 50 (Carl Zeiss MicroImaging) or DMRA (Leica) microscope and Metamorph software. Protein bands on immunoblots were visualized with HRP-labeled donkey anti-rabbit, anti-mouse, or anti-rat IgG followed by detection with chemiluminescence. For the graphical representation of modification levels in Figure 4, protein bands from immunoblots were quantified using ImageJ software.

ACCESSION NUMBERS

Sequences for CCP4 and CCP6 have been deposited in public databases with the accession numbers FN429927 and FN427928.

SUPPLEMENTAL INFORMATION

Supplemental Information includes Extended Experimental Procedures, six figures, and four tables and can be found with this article online at doi:10.1016/j.cell.2010.10.014.

ACKNOWLEDGMENTS

This work was supported by the CNRS, the Universities Montpellier 2 and 1, the Institut Curie, the Association pour la Recherche sur le Cancer (ARC) award 3140 to C.J. and awards 4892 and 7927 to A.A., the French National Research

Agency (ANR) awards 05-JCJC-0035 and 08-JCJC-0007 to C.J. and "Tyr-Tips" to A.A., the Fondation pour la Recherche Médicale (FRM) research grant DEQ20081213977, the HFSP program grant RGP 23/2008, and the EMBO Young Investigator Program grant to C.J., the La Ligue contre le cancer research grant R07Job to A.A., and the Alzheimer Forschung Initiative project 06825 to M.H. B.L. was supported by a fellowship from the La Ligue contre le Cancer and the EMBO short-term fellowship ASTF 157-2007. K.R. received two postdoctoral fellowships from the La Ligue contre le Cancer and the EMBO long-term fellowship ALTF 546-2006.

We thank L. Cotter (INSERM U836, Grenoble, France), G. Aldrian-Herrada, J. Boudeau, J.-M. Donnay, J.-C. Mazur, J. Miro (CRBM, Montpellier, France), K. Chebli, C. Jacquet, E. Jouffre (IGMM, Montpellier, France), C. Alberti, E. Belloir, H. Yu (Institut Curie, Orsay, France), V. Bäcker, J. Cau, S. DeRossi, P. Travo (RIO Imaging facility at the CRBM), and R. Holzer (University of Leipzig, Germany) for technical assistance. We are grateful to D. Job (INSERM U836, Grenoble, France) and U. Schmidt (IGMM, Montpellier, France) for instructive discussions. We are grateful to L. Lafanechère (CEA, Grenoble, France) for the kind gift of the anti-Δ2-tubulin antibody. The monoclonal antibody 12G10 developed by J. Frankel and M. Nelson was obtained from the Developmental Studies Hybridoma Bank, developed under the auspices of the NICHD, and maintained by the University of Iowa.

Received: February 2, 2010
Revised: August 13, 2010
Accepted: October 5, 2010
Published: November 11, 2010

REFERENCES

Audebert, S., Desbruyeres, E., Gruszczynski, C., Koulakoff, A., Gros, F., Denoulet, P., and Eddé, B. (1993). Reversible polyglutamylation of alpha- and beta-tubulin and microtubule dynamics in mouse brain neurons. Mol. Biol. Cell *4*, 615–626.

Berezniuk, I., Sironi, J., Callaway, M.B., Castro, L.M., Hirata, I.Y., Ferro, E.S., and Fricker, L.D. (2010). CCP1/Nna1 functions in protein turnover in mouse brain: Implications for cell death in Purkinje cell degeneration mice. Faseb J. *24*, 1813–1823.

Bobinnec, Y., Moudjou, M., Fouquet, J.P., Desbruyeres, E., Eddé, B., and Bornens, M. (1998). Glutamylation of centriole and cytoplasmic tubulin in proliferating non-neuronal cells. Cell Motil. Cytoskeleton *39*, 223–232.

Bré, M.H., de Nechaud, B., Wolff, A., and Fleury, A. (1994). Glutamylated tubulin probed in ciliates with the monoclonal antibody GT335. Cell Motil. Cytoskeleton *27*, 337–349.

Chakrabarti, L., Eng, J., Martinez, R.A., Jackson, S., Huang, J., Possin, D.E., Sopher, B.L., and La Spada, A.R. (2008). The zinc-binding domain of Nna1 is required to prevent retinal photoreceptor loss and cerebellar ataxia in Purkinje cell degeneration (pcd) mice. Vision Res. *48*, 1999–2005.

Chakrabarti, L., Zahra, R., Jackson, S.M., Kazemi-Esfarjani, P., Sopher, B.L., Mason, A.G., Toneff, T., Ryu, S., Shaffer, S., Kansy, J.W., et al. (2010). Mitochondrial dysfunction in NnaD mutant flies and Purkinje cell degeneration mice reveals a role for Nna proteins in neuronal bioenergetics. Neuron *66*, 835–847.

Eddé, B., Rossier, J., Le Caer, J.P., Desbruyeres, E., Gros, F., and Denoulet, P. (1990). Posttranslational glutamylation of alpha-tubulin. Science *247*, 83–85.

Ersfeld, K., Wehland, J., Plessmann, U., Dodemont, H., Gerke, V., and Weber, K. (1993). Characterization of the tubulin-tyrosine ligase. J. Cell Biol. *120*, 725–732.

Fernandez-Gonzalez, A., La Spada, A.R., Treadaway, J., Higdon, J.C., Harris, B.S., Sidman, R.L., Morgan, J.I., and Zuo, J. (2002). Purkinje cell degeneration (pcd) phenotypes caused by mutations in the axotomy-induced gene, Nna1. Science *295*, 1904–1906.

Gao, Y., Ye, L.H., Kishi, H., Okagaki, T., Samizo, K., Nakamura, A., and Kohama, K. (2001). Myosin light chain kinase as a multifunctional regulatory protein of smooth muscle contraction. IUBMB Life *51*, 337–344.

Herring, B.P., El-Mounayri, O., Gallagher, P.J., Yin, F., and Zhou, J. (2006). Regulation of myosin light chain kinase and telokin expression in smooth muscle tissues. Am. J. Physiol. Cell Physiol. *291*, C817–C827.

Ikegami, K., Sato, S., Nakamura, K., Ostrowski, L.E., and Setou, M. (2010). Tubulin polyglutamylation is essential for airway ciliary function through the regulation of beating asymmetry. Proc. Natl. Acad. Sci. USA *107*, 10490–10495.

Janke, C., Rogowski, K., Wloga, D., Regnard, C., Kajava, A.V., Strub, J.-M., Temurak, N., van Dijk, J., Boucher, D., van Dorsselaer, A., et al. (2005). Tubulin polyglutamylase enzymes are members of the TTL domain protein family. Science *308*, 1758–1762.

Kalinina, E., Biswas, R., Berezniuk, I., Hermoso, A., Aviles, F.X., and Fricker, L.D. (2007). A novel subfamily of mouse cytosolic carboxypeptidases. FASEB J. *21*, 836–850.

Kimura, Y., Kurabe, N., Ikegami, K., Tsutsumi, K., Konishi, Y., Kaplan, O.I., Kunitomo, H., Iino, Y., Blacque, O.E., and Setou, M. (2010). Identification of tubulin deglutamylase among Caenorhabditis elegans and mammalian cytosolic carboxypeptidases (CCPs). J. Biol. Chem. *285*, 22936–22941.

Kubo, T., Yanagisawa, H.-a., Yagi, T., Hirono, M., and Kamiya, R. (2010). Tubulin polyglutamylation regulates axonemal motility by modulating activities of inner-arm dyneins. Curr. Biol. *20*, 441–445.

Lacroix, B., van Dijk, J., Gold, N.D., Guizetti, J., Aldrian-Herrada, G., Rogowski, K., Gerlich, D.W., and Janke, C. (2010). Tubulin polyglutamylation stimulates spastin-mediated microtubule severing. J. Cell Biol. *189*, 945–954.

Mullen, R.J., Eicher, E.M., and Sidman, R.L. (1976). Purkinje cell degeneration, a new neurological mutation in the mouse. Proc. Natl. Acad. Sci. USA *73*, 208–212.

Pathak, N., Obara, T., Mangos, S., Liu, Y., and Drummond, I.A. (2007). The zebrafish fleer gene encodes an essential regulator of cilia tubulin polyglutamylation. Mol. Biol. Cell *18*, 4353–4364.

Paturle-Lafanechere, L., Eddé, B., Denoulet, P., Van Dorsselaer, A., Mazarguil, H., Le Caer, J.P., Wehland, J., and Job, D. (1991). Characterization of a major brain tubulin variant which cannot be tyrosinated. Biochemistry *30*, 10523–10528.

Paturle-Lafanechere, L., Manier, M., Trigault, N., Pirollet, F., Mazarguil, H., and Job, D. (1994). Accumulation of delta 2-tubulin, a major tubulin variant that cannot be tyrosinated, in neuronal tissues and in stable microtubule assemblies. J. Cell Sci. *107*, 1529–1543.

Redeker, V., Frankfurter, A., Parker, S.K., Rossier, J., and Detrich, H.W., 3rd. (2004). Posttranslational modification of brain tubulins from the antarctic fish Notothenia coriiceps: reduced C-terminal glutamylation correlates with efficient microtubule assembly at low temperature. Biochemistry *43*, 12265–12274.

Regnard, C., Desbruyeres, E., Denoulet, P., and Eddé, B. (1999). Tubulin polyglutamylase: isozymic variants and regulation during the cell cycle in HeLa cells. J. Cell Sci. *112*, 4281–4289.

Regnard, C., Desbruyeres, E., Huet, J.C., Beauvallet, C., Pernollet, J.C., and Eddé, B. (2000). Polyglutamylation of nucleosome assembly proteins. J. Biol. Chem. *275*, 15969–15976.

Rodriguez de la Vega, M., Sevilla, R.G., Hermoso, A., Lorenzo, J., Tanco, S., Diez, A., Fricker, L.D., Bautista, J.M., and Aviles, F.X. (2007). Nna1-like proteins are active metallocarboxypeptidases of a new and diverse M14 subfamily. FASEB J. *21*, 851–865.

Rüdiger, M., Plessman, U., Kloppel, K.D., Wehland, J., and Weber, K. (1992). Class II tubulin, the major brain beta tubulin isotype is polyglutamylated on glutamic acid residue 435. FEBS Lett. *308*, 101–105.

Rusconi, F., Potier, M.C., Le Caer, J.P., Schmitter, J.M., and Rossier, J. (1997). Characterization of the chicken telokin heterogeneity by time-of-flight mass spectrometry. Biochemistry *36*, 11021–11026.

Smith, A.F., Bigsby, R.M., Word, R.A., and Herring, B.P. (1998). A 310-bp minimal promoter mediates smooth muscle cell-specific expression of telokin. Am. J. Physiol. *274*, C1188–C1195.

Suryavanshi, S., Edde, B., Fox, L.A., Guerrero, S., Hard, R., Hennessey, T., Kabi, A., Malison, D., Pennock, D., Sale, W.S., et al. (2010). Tubulin glutamylation regulates ciliary motility by altering inner dynein arm activity. Curr. Biol. *20*, 435–440.

Vallee, R.B. (1986). Reversible assembly purification of microtubules without assembly-promoting agents and further purification of tubulin, microtubule-associated proteins, and MAP fragments. Methods Enzymol. *134*, 89–104.

van Dijk, J., Rogowski, K., Miro, J., Lacroix, B., Eddé, B., and Janke, C. (2007). A targeted multienzyme mechanism for selective microtubule polyglutamylation. Mol. Cell *26*, 437–448.

van Dijk, J., Miro, J., Strub, J.-M., Lacroix, B., van Dorsselaer, A., Eddé, B., and Janke, C. (2008). Polyglutamylation Is a Post-translational Modification with a Broad Range of Substrates. J. Biol. Chem. *283*, 3915–3922.

Wang, T., and Morgan, J.I. (2007). The Purkinje cell degeneration (pcd) mouse: an unexpected molecular link between neuronal degeneration and regeneration. Brain Res. *1140*, 26–40.

Wang, T., Parris, J., Li, L., and Morgan, J.I. (2006). The carboxypeptidase-like substrate-binding site in Nna1 is essential for the rescue of the Purkinje cell degeneration (pcd) phenotype. Mol. Cell. Neurosci. *33*, 200–213.

Wloga, D., Dave, D., Meagley, J., Rogowski, K., Jerka-Dziadosz, M., and Gaertig, J. (2009). Hyperglutamylation of tubulin can either stabilize or destabilize microtubules in the same cell. Eukaryot. Cell *9*, 184–193.

Wolff, A., de Nechaud, B., Chillet, D., Mazarguil, H., Desbruyeres, E., Audebert, S., Eddé, B., Gros, F., and Denoulet, P. (1992). Distribution of glutamylated alpha and beta-tubulin in mouse tissues using a specific monoclonal antibody, GT335. Eur. J. Cell Biol. *59*, 425–432.